THE ASTROPHYSICAL JOURNAL, 625:L103–L106, 2005 June 1

DISCOVERY OF STRONG LENSING BY AN ELLIPTICAL GALAXY AT $z = 0.0345$[1]

RUSSELL J. SMITH,[2] JOHN P. BLAKESLEE,[3] JOHN R. LUCEY,[4] AND JOHN TONRY[5]

Received 2005 March 3; accepted 2005 April 20; published 2005 May 3

ABSTRACT

We have discovered strong gravitational lensing by the galaxy ESO 325-G004, in images obtained with the Advanced Camera for Surveys on the *Hubble Space Telescope*. The lens galaxy is a boxy group-dominant elliptical at $z = 0.0345$, making this the closest known galaxy-scale lensing system. The lensed object is very blue ($B - I_C \approx 1.1$), and forms two prominent arcs and a less extended third image. The Einstein radius is $R_{\rm Ein} = 1.9$ kpc (~3″ on the sky), much smaller than the lens galaxy effective radius of 8.5 kpc. Assuming a high redshift for the source, the mass within $R_{\rm Ein}$ is $1.4 \times 10^{11}\ M_\odot$, and the mass-to-light ratio is 1.8 $(M/L)_{\odot,I}$. The equivalent velocity dispersion is $\sigma_{\rm lens} = 310$ km s^{-1}, in excellent agreement with the measured stellar dispersion $\sigma_v = 320$ km s^{-1}. Modeling the lensing potential with a singular isothermal ellipse (SIE), we find close agreement with the light distribution. The best-fit SIE model reproduces the ellipticity of the lens galaxy to ~10%, and its position angle within 1°. The model predicts the broad features of the arc geometry as observed; the unlensed magnitude of the source is estimated at $I_C \sim 23.75$. We suggest that ~60 similarly massive elliptical galaxies within $z < 0.1$ will exhibit such a luminous, multiply imaged source.

Subject headings: galaxies: elliptical and lenticular, cD — gravitational lensing

1. INTRODUCTION

Gravitational lensing of background sources can yield valuable information on the mass profiles of galaxies, groups, and clusters. In contrast to other methods, lensing constraints are independent of assumptions about the dynamical or hydrodynamic state of tracer material (e.g., stars, galaxies, X-ray gas). On galaxy scales, lensing helps to lift the degeneracy between the potential and the orbital anisotropy that plagues dynamical mass estimates. For distant galaxies, lensing constrains the mass enclosed at large radii, beyond the reach of stellar dynamical studies (e.g., Treu & Koopmans 2004).

The optimal configuration for lensing is with the deflecting potential at half the distance to the source. Hence, lensing is usually observed for systems at intermediate redshift, $z \sim 0.3$, where the number of potential background sources is very large. At low redshifts ($z \lesssim 0.1$), strong-lensing systems are rare. On cluster scales, a number of lensed arcs have been discussed (e.g., Blakeslee et al. 2001). The nearest known galaxy-scale strong-lensing system, prior to this Letter, was Q2237+0305 (Huchra et al. 1985), a four-image QSO lensed by a $z = 0.039$ spiral. Among galaxy lenses with extended arcs, the lowest known lens redshift is $z = 0.205$, for SDSS 1402+6321 (Bolton et al. 2005). This system was discovered on the basis of anomalous emission lines in the lens galaxy spectrum. A more direct approach to finding extended arcs is, of course, through imaging observations. Blakeslee et al. (2004) have discussed the excellent prospects for serendipitous discovery of strong lens galaxies with the Advanced Camera for Surveys (ACS) on the *Hubble Space Telescope*.

In this Letter, we report the ACS discovery of a new galaxy-scale lens, with multiple extended images, at $z = 0.0345$. To our knowledge, the elliptical galaxy ESO 325-G004 is the nearest known strong-lensing galaxy and provides for the first time a low-redshift analog of distant galaxy-scale arc systems.

We adopt the *WMAP* cosmological parameters, i.e., $H_0 = 71$ km s^{-1} Mpc^{-1}, $\Omega_m = 0.27$, and $\Omega_\Lambda = 0.73$ (Bennett et al. 2003).

2. THE LENS GALAXY ESO 325-G004

The massive boxy elliptical galaxy ESO 325-G004 ($13^{\rm h}43^{\rm m}33\overset{\rm s}{.}20$, $-38°10'33\overset{''}{.}6$) lies at the center of the poor Abell cluster S0740 (Abell et al. 1989) and is probably the dominant galaxy of that group. The galaxy has a radial velocity $cz = 10{,}420$ km s^{-1} in the cosmic microwave background frame (Smith et al. 2000), corresponding to an angular scale of 0.678 kpc arcsec^{-1}. The Galactic extinction is $E(B - V) = 0.06$ (Schlegel et al. 1998). The stellar velocity dispersion of ESO 325-G004 was measured by Smith et al. (2000), within an aperture 3.8×3.0 arcsec^2; the average of their two measurements is $\sigma_v = 320 \pm 7$ km s^{-1}. Smith et al. (2001) report the effective radius as $R_{\rm eff} = 12\overset{''}{.}5$ (8.5 kpc) from *R*-band imaging.

Understanding the environment of the lens galaxy can be critical for the correct interpretation of lensing constraints. Figure 1 shows the projected galaxy density around ESO 325-G004 and the distribution of published redshifts. Although not complete, the redshift data suggest that S0740 is distinct from the neighboring cluster A3570 (~40′ away and with a mean redshift ~1000 km s^{-1} larger).

ESO 325-G004 was observed with ACS in 2005 January, as part of our program measuring surface brightness fluctuations in the Shapley foreground region. The total integration times were 18,882 s in F814W (22 individual exposures) and 1101 s (three exposures) in F475W. The frames were combined using MULTIDRIZZLE in STSDAS to yield the stacks used in this study (Fig. 2). Inspection of the images revealed two long, narrow arcs at ~3″ separation from the galaxy center (Fig. 3). A third object, less obviously distorted, is present at similar radius. The arcs are prominent even in the much shallower F475W exposure (Fig. 3*a*), due to favorable color con-

[1] Based on observations made with the NASA/ESA *Hubble Space Telescope*, obtained at the Space Telescope Science Institute, which is operated by the Association of Universities for Research in Astronomy, Inc., under NASA contract NAS 5-26555. These observations are associated with program 10429.

[2] Department of Physics, University of Waterloo, 200 University Avenue West, Waterloo, ON N2L 3G1, Canada; rjsmith@astro.uwaterloo.ca.

[3] Department of Physics and Astronomy, Johns Hopkins University, 3400 North Charles Street, Baltimore, MD 21218; jpb@pha.jhu.edu.

[4] Department of Physics, University of Durham, Durham DH1 3LE, UK; john.lucey@durham.ac.uk.

[5] Institute for Astronomy, University of Hawaii, 2680 Woodlawn Drive, Honolulu, HI 96822-1897; jt@ifa.hawaii.edu.

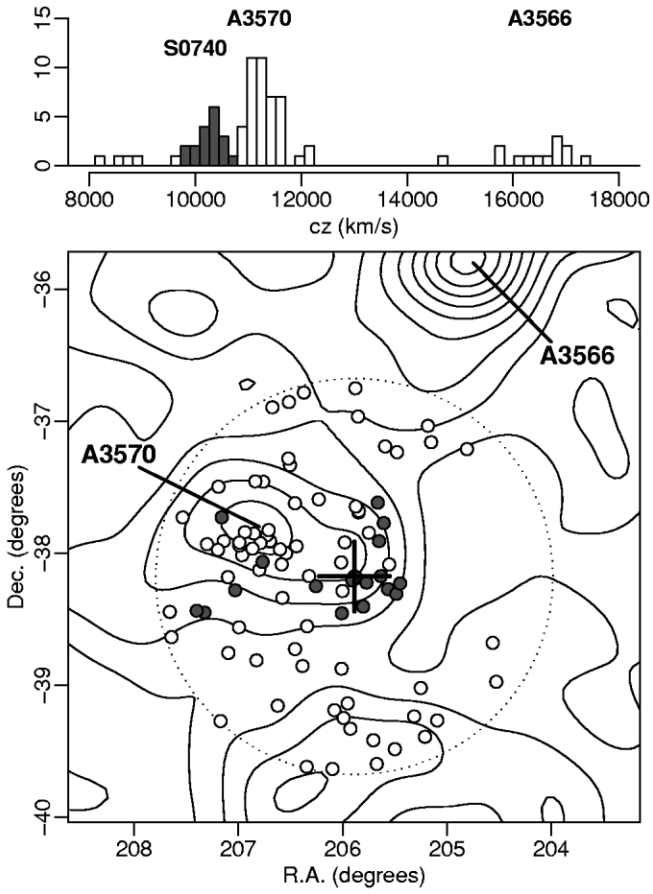

FIG. 1.—Environment of the lensing galaxy. The main figure shows contours of projected galaxy density from the 2MASS extended source catalog. The small circles mark galaxies with measured redshifts in the NASA Extragalactic Database, within 1.°5 of ESO 325-G004. Galaxies with redshifts within 500 km s^{-1} of ESO 325-G004 are shaded. The histogram above shows the same redshifts, with the same redshift interval highlighted.

trast between the blue arcs and the red light of the foreground elliptical galaxy.

For a preliminary photometric analysis of the lens galaxy, we applied IRAF tasks based on the ellipse-fitting algorithm of Jedrzejewski (1987). The surface photometry model includes the c_4 Fourier coefficient, which is necessary to describe the strong boxiness of the isophotes. All other high-order Fourier terms were forced to zero. The luminosity profile follows a $R^{1/4}$ law out to at least $\sim 1'$ ($\sim 5R_{\rm eff}$). Transformed to the Johnson/Cousins system (following Sirianni et al. 2005), and correcting for extinction and *k*-dimming, the color is $B - I_{\rm C} \approx 2.5$, typical for an old, metal-rich stellar population. At the radius of the arcs, the isophotal position angle is 68°, and the ellipticity $e = 1 - b/a \approx 0.25$.

Although the arcs are seen clearly in the original images (Fig. 3*a*), their visibility is enhanced by subtracting a model for the lens galaxy light. We have explored a number of approaches to this subtraction. The simplest method uses the ellipse+c_4 fits described above, subtracting independent models for the F814W and F475W images. The resulting F814W residual image is shown in Figure 3*b*. This method leaves a strong spoke pattern; there is also a risk of introducing tangential residuals unrelated to lensing. A more robust approach is to use the color contrast between the arcs and the galaxy, subtracting a scaled version of the F814W image from the

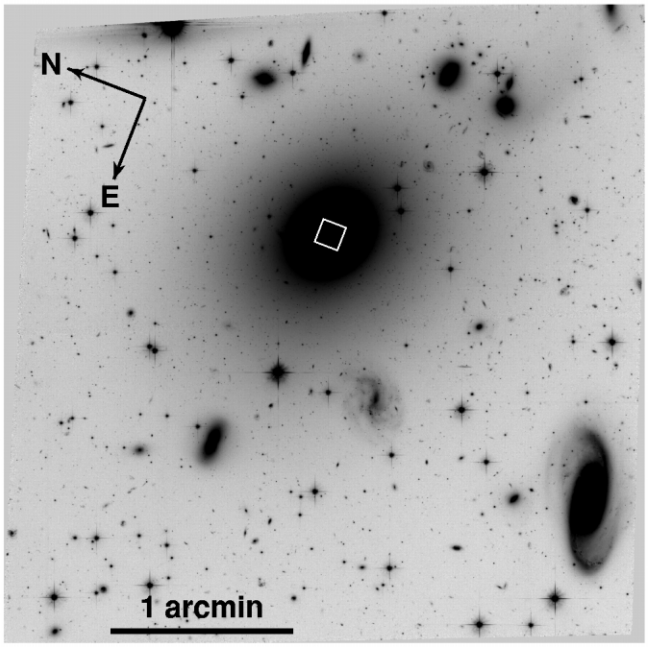

FIG. 2.—Deep (18,882 s) F814W image of ESO 325-G004 and the surrounding field. The white square indicates the central 8 × 8 $\rm arcsec^2$ region covered by Fig. 3.

F475W image. The color residual image (Fig. 3*c*) is limited by noise from the shallow F475W exposure but is systematically very clean; in particular, the spoke pattern and many of the point sources are removed.

In § 3, we will show that the observed geometry of arcs "A," "B," and "C" is indeed consistent with a single background source lensed by an elliptical potential. We have determined approximate magnitudes and colors for the arcs, based on the residual images, as summarized in Table 1. In particular, note that the arcs have consistent colors, with $B - I_{\rm C} = 1.10 \pm 0.05$ (extinction-corrected). Such a blue color can be reproduced with star-forming spectral templates at $z \lesssim 0.45$, with [O II λ3727] contributing to the F475W flux. The arcs have irregular surface brightness distributions, with numerous "knots," suggestive of star-forming regions. In B we can identify at least seven knots, while A shows a symmetric structure as expected for a two-image arc, and C appears double.

3. MASS-TO-LIGHT RATIO FROM LENSING

We have used simple mass models to test the assumption that all three images are generated by gravitational lensing and to derive initial estimates for the mass enclosed within the arcs. To test parameterized forms for the lensing potential, we applied the "curve-fitting" method as implemented within the GRAVLENS/LENSMODEL software (Keeton 2001). This method takes as input a set of points on each observed arc and optimizes a lensing potential that maps points from each curve to counterimages on the other curves. The input curves were obtained by manually tracing arcs A, B, and C. To determine a well-defined Einstein radius for an elliptical potential, Rusin et al. (2003) have suggested a scheme based on fitting a singular isothermal sphere (SIS) plus external shear. The model has three parameters, the SIS Einstein radius, and the magnitude and position angle of the shear. This parameter space was explored

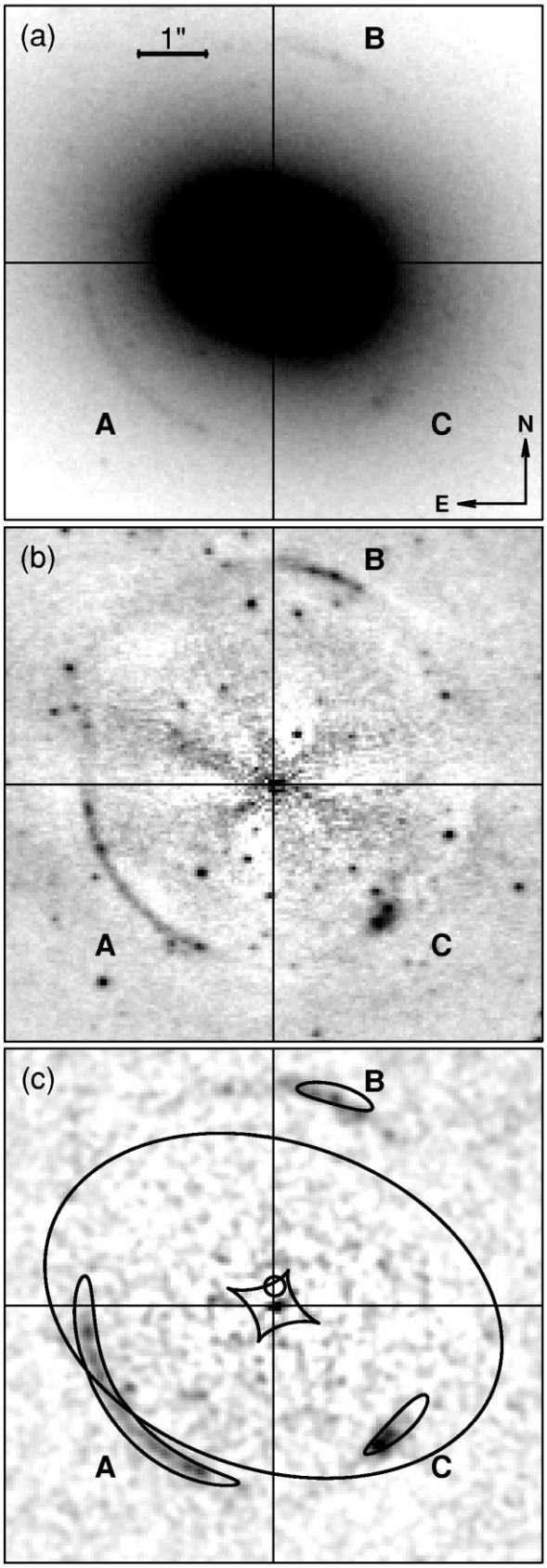

FIG. 3.—Observations and models of lensing in ESO 325-G004. Panel *a* shows the 1101 s F475W image, with color map optimized to show the arcs. In panel *b*, the 18,882 s F814W image is shown after subtracting a smooth boxy-elliptical profile model. In panel *c*, we show the color-subtracted image, with results from a lensing model for a singular isothermal ellipse (see text).

TABLE 1

PROPERTIES OF THE ARCS

ID	Radius[a]	Length[a]	F814W[b]	F475W[b]	$(B - I_C)_{corr}$[c]
A	2.8	3.4	22.06	22.93	1.07
B	3.4	1.5	22.92	23.88	1.21
C	2.6	0.9	22.61	23.45	1.03

[a] Radius and length (in arcseconds) of an annular segment bounding the $\mu_{F814W} = 23$ mag arcsec^{-1} isophote, as used for the photometry.
[b] Integrated magnitude and color, on the Vega system, within the annular segment.
[c] Johnson/Cousins, corrected for Galactic extinction.

using a combination of grid-search and simplex optimization methods.

The best SIS+shear fit yields $R_{Ein} \approx 2\farcs85$ (1.93 kpc or 0.23 R_{eff}). From this we can determine the mass interior to R_{Ein} to be $M_{Ein} \approx 1.4(D_s/D_{ls}) \times 10^{11}\ M_\odot$. Here D_s is the angular-diameter distance to the source, and D_{ls} the angular-diameter distance between lens and source. The enclosed mass measurement thus depends on the source redshift, which is as yet unknown (but see below). For a given lens, the source is most likely to be at high redshift, where the surface density of potential sources is very large. In this section, we consider the limiting case of a distant source, such that $D_s/D_{ls} \approx 1$. The observed magnitudes interior to R_{Ein} are F814W = 13.5 and F475W = 15.6. Transforming these to Johnson/Cousins bandpasses following Sirianni et al. (2005), we have $I_C = 12.7$ and $B = 15.1$ (corrected for extinction and *k*-dimming). Converting to luminosities we have $L_{Ein,I_C} = 8.0 \times 10^{10}\ L_{\odot,I_C}$ and $L_{Ein,B} = 3.0 \times 10^{10}\ L_{\odot,B}$, and the mass-to-light ratios at the Einstein radius are $\Upsilon_{Ein,I_C} = 1.8\ (M/L)_{\odot,I_C}$ and $\Upsilon_{Ein,B} = 4.7\ (M/L)_{\odot,B}$. Such values are typical for stellar mass-to-light ratios in old populations. Thus, the mass budget within the Einstein radius appears to be dominated by the observed stellar mass.[6] The SIS mass model yields $\sigma_{SIS} = 310$ km s^{-1}, in excellent agreement with the measured stellar velocity dispersion.

Considering the morphology of the galaxy, and the expectation that the mass within R_{Ein} will be dominated by stars, a more realistic model for the lensing potential is the singular isothermal ellipse (SIE; e.g., Korman et al. 1994). In fitting the SIE model, we force the center of the potential to align with the observed galaxy, but we allow the mass normalization, position angle, and ellipticity to vary. Formally, the best-fitting model has ellipticity $e = 0.28$ with position angle 68°, very similar to the equivalent parameters for the galaxy light. Figure 3*c* shows the results of this best-fitting SIE model. The reconstructed source position is ~0.″3 north of the lens center (*small circle*) and likely straddles the inner "astroid" caustic of the lens model (*inner cusped curve*). The figure shows the predicted image locations for such a source. Qualitatively, the SIE potential reproduces the broad features of the observed geometry and confirms image C as a counterimage of A and B. The long arc A comprises two images crossing the critical curve (*outer ellipse*). While broadly successful, it is also clear that the model does not match the data perfectly at a more detailed level. In particular, the SIE does not match the relative lengths of the three observed arcs. For C, moreover, the model predicts a position displaced toward B, relative to the observed location. To improve the reconstruction, more sophisticated mod-

[6] Given independent information on the stellar population (e.g., from spectroscopic line indices), this result could yield an upper limit on the mass contribution from dark matter associated with ESO 325-G004 and/or the surrounding cluster S0740.

els could take into account the intrinsic morphology of the source, the boxiness of the lens galaxy, and a possible external shear term.

4. DISCUSSION

It is interesting to consider whether the lensing configuration observed in ESO 325-G004 is intrinsically unusual or whether many other nearby galaxies might reveal such bright arcs when observed in sufficient detail. The cross section for four-image lensing under the SIE mass model is $\sim$1 arcsec^2, i.e., roughly the area of the astroid caustic on the source plane. The estimated magnification factors for the separated arcs B and C are $\sim$4, suggesting that the unlensed magnitude of the source is $I_C \sim 23.75$. To this limit, the integrated *I*-band galaxy counts are $\sim 10^5$ deg^{-2} (Postman et al. 1998), so the probability that a given galaxy has such a bright background source aligned for quadruple imaging is $\sim$0.6%. To estimate the total number of massive galaxies available to serve as low-redshift lenses, we use the Two Micron All Sky Survey (2MASS) *J*-band luminosity function of Cole et al. (2001). ESO 325-G004 has $M_J - 5 \log h = -24.16$, and thus a luminosity $\sim 7L_J^\star$. Integrating the luminosity function, parameterized as a Schechter function, the space density of galaxies above $7L_J^\star$ is 2.8×10^{-5} Mpc^{-3} (for $h = 0.71$). This density implies $\sim 10^4$ galaxies, at least as luminous as ESO 325-G004, within $z = 0.1$. Combining these estimates, we find the total expected number of "similar" low-redshift lens systems to be $\sim$60, with only $\sim$3 at the distance of ESO 325-G004 or closer.

As noted above, the lens model normalization depends on the source redshift, through the factor D_s/D_{ls}. We have reexamined the raw spectra obtained by Smith et al. (2000) at the Anglo-Australian Telescope (AAT), which cover the range 4925–5740 Å, with slit intercepting arc C. No anomalous emission lines are seen at the expected position of the arc, which at face value suggests $z_{\rm src} > 0.54$ and $z_{\rm src} < 0.32$ (absence of [O II λ3727]), but also $z_{\rm src} > 0.15$ (absence of [O III λ5007] and Hβ). Over the redshift interval 0.15–0.32, the lensing mass correction factor D_s/D_{ls} ranges from 1.30 to 1.13. It is, however, quite possible that the exposures were too short (600 s), and the slit too wide (3″), to detect emission from the arc against the high background of the lens galaxy.

Finally, we note that our images show four extremely faint tangential arc candidates at greater separation from ESO 325-G004 (radius 9.″4, at position angles $-95°$, 90°, $-35°$, and 150°). The surface brightness of these features is very low ($\gtrsim$24.5 mag arcsec^{-2} in *I*). If confirmed, the outer arcs could provide additional constraints on the mass distribution at larger radius and on the relative contribution of the group potential to the lensing mass.

5. CONCLUSIONS

We have discovered strong gravitational lensing by the elliptical galaxy ESO 325-G004, which at $z = 0.0345$ is the nearest known galaxy-scale lens. The multiply imaged background source appears to be a star-forming galaxy, with prominent substructure. If the source is very distant, the arc radius is consistent with a stellar-dominated mass-to-light ratio within radius $\sim \frac{1}{4} R_{\rm eff}$. An elliptical isothermal mass model recovers the position angle and ellipticity of the galaxy, independent of the observed luminosity. The best-fit mass scale is consistent with the measured stellar velocity dispersion. Future modeling of the system should incorporate structural information from the clumpy arc morphology. We intend to obtain integral-field spectroscopy for ESO 325-G004, with 8 m–class telescopes, to secure the source redshift and enclosed mass estimate. Additionally, these observations will yield extended stellar dynamics for the lens galaxy and enable us to perform high-contrast imaging of the arcs by emission-line mapping.

R. J. S. thanks Mike Hudson and Laura Parker for useful discussions about this work, and the Anglo-Australian Observatory for retrieving the raw AAT spectra of ESO 325-G004. This research has made use of the NASA/IPAC Extragalactic Database (NED), which is operated by the Jet Propulsion Laboratory, California Institute of Technology, under contract with the National Aeronautics and Space Administration. This publication makes use of data products from the Two Micron All Sky Survey, which is a joint project of the University of Massachusetts and the Infrared Processing and Analysis Center/California Institute of Technology, funded by the National Aeronautics and Space Administration and the National Science Foundation.

REFERENCES

Abell, G. O., Corwin, H. G., Jr., & Olowin, R. P. 1989, ApJS, 70, 1
Bennett, C. L., et al. 2003, ApJS, 148, 1
Blakeslee, J. P., Metzger, M. R., Kuntschner, H., & Côté, P. 2001, AJ, 121, 1
Blakeslee, J. P., et al. 2004, ApJ, 602, L9
Bolton, A. S., Burles, S., Koopmans, L. V. E., Treu, T., & Moustakas, L. A. 2005, ApJ, 624, L21
Cole, S. M., et al. 2001, MNRAS, 326, 255
Huchra, J., Gorenstein, M., Kent, S., Shapiro, I., Smith, G., Horine, E., & Perley, R. 1985, AJ, 90, 691
Jedrzejewski, R. I. 1987, MNRAS, 226, 747
Keeton, C. R. 2001, preprint (astro-ph/0102340)
Kormann, R., Schneider, P., & Bartelmann, M. 1994, A&A, 284, 285
Postman, M., Lauer, T. R., Szapudi, I., & Oegerle, W. 1998, ApJ, 506, 33
Rusin, D., Kochanek, C. S., & Keeton, C. R. 2003, ApJ, 595, 29
Schlegel, D. J., Finkbeiner, D. P., & Davis, M. 1998, ApJ, 500, 525
Sirianni, M., et al. 2005, PASP, submitted
Smith, R. J., Lucey, J. R., Hudson, M. J., Schlegel, D. J., & Davies, R. L. 2000, MNRAS, 313, 469
Smith, R. J., Lucey, J. R., Schlegel, D. J., Hudson, M. J., Baggley, G., & Davies, R. L. 2001, MNRAS, 327, 249
Treu, T., & Koopmans, L. V. E. 2004, ApJ, 611, 739